Cu-Zn disorder in stoichiometric and non-stoichiometric Cu_2ZnSnS_4/$Cu_2ZnSnSe_4$

Cite as: AIP Advances 9, 035248 (2019); doi: 10.1063/1.5090804
Submitted: 30 January 2019 • Accepted: 13 March 2019 •
Published Online: 25 March 2019

Yi-Feng Zheng,[1,2] Ji-Hui Yang,[1] and Xin-Gao Gong[1,2,a)]

AFFILIATIONS

[1]Department of Physics, Key Laboratory for Computational Science (MOE), State Key Laboratory of Surface Physics, Fudan University, Shanghai 200433, China
[2]Collaborative Innovation Center of Advanced Microstructures, Nanjing University, 210093 Jiangsu, China

[a)]Corresponding email address: xggong@fudan.edu.cn

ABSTRACT

Cu-Zn disorder is unavoidable but plays an important role in high-efficiency Cu_2ZnSnS_4 and $Cu_2ZnSnSe_4$ solar cells. Using the cluster expansion method along with Monte Carlo (MC) simulations, we study the Cu-Zn disorder, considering cases both with and without vacancies. We find that the 2a, 2c, and 2d Wyckoff sites all show order-disorder transitions for both cases, in agreement with recent experiments supporting disorder at all 2a, 2c and 2d sites, but, in contrast to early experiments, supporting Cu-Zn disorder only at 2c and 2d sites. Below the transition temperature in non-stoichiometric cases, we find that excess Zn prefers to occupy 2c over 2a sites due to the greater similarity of 2c sites to 2d sites. Such site preferences indicate that Cu-Zn occupations exhibit some new kind of ordering rather than randomly distributed at 2a and 2c sites. We find that while Cu-Zn disorder reduces the band gap, the site preferences in non-stoichiometric samples increase the band gaps by suppressing Cu-Zn disorder. Generally, lowering annealing temperatures, while increasing Zn and vacancies, will lead to larger band gaps.

I. INTRODUCTION

In the development of thin-film photovoltaic technology, Cu_2ZnSnS_4 (CZTS) and $Cu_2ZnSnSe_4$ (CZTSe) with multi-cations have been considered to be promising absorber materials, containing only non-toxic and earth-abundant elements. However, the best power conversion efficiency[1] of 12.6% for $Cu_2ZnSn(S,Se)_4$ is still low compared with other commercially viable absorber materials such as CdTe (22.1%)[2] and $Cu(In,Ga)Se_2$ (22.6%).[3] One main reason for the low efficiency is the large open-circuit voltage deficit.[4] Among all possible factors causing reduction of the open-circuit voltage, one common view is that cation disorder plays an important role, by causing electrostatic potential fluctuations[5–7] which decrease the band gap of the absorber.

It is well known that cations are arranged systematically in perfect CZTS and CZTSe compounds with a kesterite ground state structure[8] at zero temperature, with Cu cations residing at the Wyckoff positions of 2a and 2c, Zn at 2d and Sn at 2b, as illustrated in Fig. 1(a). However, at finite temperatures, the entropy tends to mix cations with formations of defects such as antisites, and when the concentration of defects is large enough, with many neighboring antisites, it is known as cation disordering. Cu-Zn antisite defects have very low formation energies due to the size similarity of Cu and Zn cations, while other defects involving Sn have higher formation energies.[9–11] Exploration of Cu-Zn-Sn disorder in all the cationic sites[12] has also demonstrated that Cu-Zn disorder dominates at the growth temperatures and Sn only gets involved in the disorder at much higher temperatures. Experimentally, an order-disorder transition with a critical temperature of around 533 K in CZTS thin films was revealed using near-resonant Raman scattering.[13] Such a transition has been further confirmed by other experimental tools such as neutron scattering[14] in CZTS, photoluminescence in CZTSe[5] and electroreflectance in $Cu_2ZnSn(S,Se)_4$.[6] While these previous experiments indicated Cu-Zn disorder just in the Cu-Zn plane (2c and 2d sites) as illustrated in Fig. 1(b), recent high-resolution neutron diffraction[15] and anomalous x-ray diffraction[16] studies suggested that the 2a site showed disorder equal to or greater than the 2c site. Theoretically, Cu-Zn disorder has been studied[12,17] in stoichiometric CZTS using the cluster expansion method[18] and Monte Carlo simulations (MC), where energies, heat capacities and

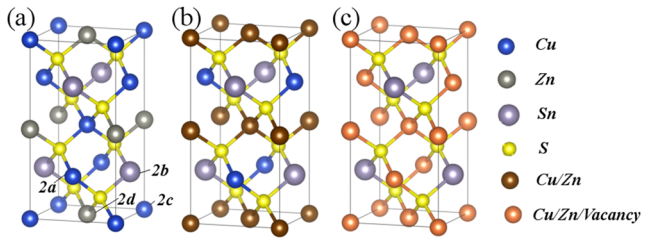

FIG. 1. (a) Perfect kesterite structure of CZTS, with Cu at the Wyckoff positions of 2a and 2c, Zn at 2d and Sn at 2b, (b) Disorder only in the Cu-Zn plane (2c and 2d), (c) Cu-Zn-vacancy disorder at 2a, 2c and 2d.

correlation functions as functions of temperature are presented to reveal the experimentally observed order-disorder transition. In contrast to experimental findings of Cu/Zn disorder at preferable sites (2c and 2d sites), these works generally supported the picture that Cu-Zn cations were disordered at all Cu/Zn sites (2a, 2c, and 2d sites) above the transition temperature. Although it was claimed[12] that complete disorder at 2a, 2c and 2d sites was revealed, the conclusion did not match their simulated curves as well as could be hoped. The signatures for the disorder from the simulated quantities, e.g. energies and correlation functions, were not very straightforward to show the detailed occupation at each site. Consequently, a clearer demonstration is needed to illustrate the disorder feature at the 2a site and resolve the discrepancies of the experimental and theoretical studies.

In fact, previous simulations of Cu-Zn disorder in stoichiometric samples only provided limited information. As is well known, Cu poor and Zn rich is the best growth condition for achieving the highest solar cell efficiency[1,19] and experimental CZTS and CZTSe samples are often non-stoichiometric with vacancies present. The structure with Cu, Zn and vacancies at all Cu-Zn sites is illustrated in Fig. 1(c). One can easily understand that the existence of vacancies would affect the disordering of various defects and also change the properties of the materials. For example, A-type complexes ($Zn_{Cu}^{+} + V_{Cu}^{-}$) are beneficial for a band gap increase.[20,21] Unfortunately, this has not been considered in previous theoretical studies of the Cu-Zn disorder. Therefore, it is worth exploring Cu-Zn disorder in both stoichiometric and non-stoichiometric samples including the effect of vacancies.

In this letter, using the cluster expansion method[22] and MC simulations,[23] we investigate the Cu-Zn disorder at Cu-Zn sites (2a, 2c and 2d) in both stoichiometric and non-stoichiometric CZTS and CZTSe. Through analyzing the structures in MC simulations, we explicitly display the temperature evolution of site occupations for each kind of atom, which presents a clear picture of the order-disorder transition and can be directly compared with experiments. For both stoichiometric and non-stoichiometric samples, 2a sites shows disorder above the transition temperature. Below the transition temperature, non-stoichiometry with vacancies causes a new kind of ordering, in which excess Zn prefers occupying 2c sites over 2a sites due to the greater similarity of the 2c site environment with that of 2d sites. Since typical samples are grown below the transition temperature to achieve higher order and larger band gaps, such a site preference is important for understanding the structural feature of experimental samples. Based on the site occupation information from MC simulations, we estimate the band gaps of samples annealed at different temperatures. We find that larger band gaps can be obtained with lower annealing temperatures, less Cu, more Zn and more vacancies, in good agreement with experiments.

II. COMPUTATIONAL METHODS

The cluster expansion method[22] describes the energy of a structure as a function of atomic occupations at certain sites. The Hamiltonian for the multicomponent alloy is

$$E(\sigma) = \sum_{\alpha} m_{\alpha} J_{\alpha} \langle \Gamma_{\alpha'}(\sigma) \rangle_{\alpha}, \quad (1)$$

where α denotes the cluster type, m_{α} is the multiplicities indicating the number of clusters equivalent by symmetry and the average is over all clusters that are equivalent by symmetry. $\Gamma_{\alpha'}(\sigma)$ are the cluster functions properly selected to form a complete orthogonal basis.[22] J_{α} are the effective cluster interactions obtained by fitting the energies of alloy structures calculated by first-principles methods. These alloy structures include both stoichiometric and non-stoichiometric CZTS (or CZTSe in a separate calculation), where Cu, Zn or a vacancy can occupy the original 2a, 2c or 2d sites. The valences of the atoms, which are +1 for Cu and +2 for Zn, are preserved. Cluster expansion is carried out by the ATAT package[24] and first-principles calculations are performed with VASP.[25,26] The projector augmented-wave (PAW)[27,28] method and the Perdew-Burke-Ernzerhof (PBE)[29] exchange correlation functional are adopted. For the relaxations of the alloy structures, we use an energy cutoff of 400 eV, a Γ-centered k-point mesh with a density of 1000 k-points per reciprocal atom and the atomic positions are relaxed until the forces are below 0.01 eV/Å. Using the cluster expansion energy, MC simulations in a canonical ensemble are performed by ATAT[23] with a supercell consisting of 17496 alloy sites (46656 atoms in total). For each given Cu:Zn:vacancy proportion, the system starts from a random structure at 1005 K, slowly cooling down to 55 K, keeping the proportion fixed in a canonical ensemble. At each temperature, the system is simulated until the average energy converges.[23]

III. RESULTS AND DISCUSSIONS

A. Temperature evolution of site occupations in CZTS

Three cases with different Cu:Zn:vacancy proportions are considered here: (1) f_{Cu}=2/3, f_{Zn}=1/3, (2) f_{Cu}=0.58, f_{Zn}=0.38, (3) f_{Cu}=0.50, f_{Zn}=0.42, where f_{Cu} means the overall proportion of Cu in 2a, 2c and 2d sites and f_{Zn} applies in the same manner. Note that (1) is stoichiometric Cu_2ZnSnS_4 while (2) and (3) are Cu poor and Zn rich cases, which correspond to the growth conditions achieving the highest solar cell efficiency[1,19] in experiments. Comparing the structures in MC simulations with the original kesterite structure, we can extract the site occupations of Cu, Zn and vacancies at 2a, 2c and 2d sites. As can be directly observed in the temperature evolutions of site occupations (Fig. 2), order-disorder transitions take place for all the cases discussed, with transition temperatures of around 500 K, close to the experimental observations.

The first obvious feature is that, above the transition temperature, all sites including 2a, 2c, and 2d sites exhibit Cu-Zn disorder, which confirms the recent experiments[15,16] and also agrees with other theoretical research.[12,17] However, a more careful

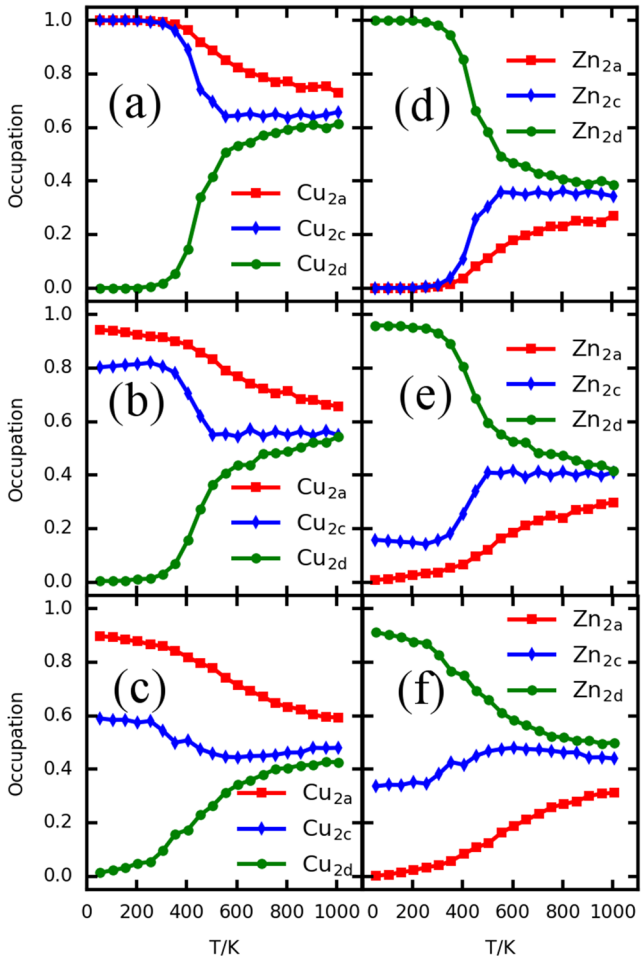

FIG. 2. Temperature evolutions of site occupations for Cu and Zn in CZTS. (a), (b) and (c) are the Cu occupations in (1) f_{Cu}=2/3, f_{Zn}=1/3 for stoichiometric sample, (2) f_{Cu}=0.58, f_{Zn}=0.38 and (3) f_{Cu}=0.50, f_{Zn}=0.42 for non-stoichiometric samples, respectively. (d), (e) and (f) are the corresponding Zn occupations. The 2a, 2c and 2d site occupations are denoted by red squares, blue diamonds and green circles respectively, which are obtained from simulated data. Lines are guides for the eye.

examination reveals that 2a sites in the Cu-Sn plane are occupied by less Zn compared to 2c and 2d sites in the Cu-Zn plane, indicating the degree of disorder at 2a sites is less than that at 2c and 2d sites. At the same time, 2c and 2d sites are almost indistinguishably disordered above the transition temperature. Such site preferences can be understood from the local environments. When the Cu and Zn at 2c and 2d sites in the Cu-Zn plane all exchange positions, the perfect kesterite structure is restored due to symmetry. Thus 2c and 2d sites are more similar and the degree of disorder is larger than that of the 2a site. Our present study shows that the picture of completely random occupations at 2a, 2c and 2d sites is not accurate and indicates an intermediate configuration of Cu-Zn disorder in CZTS, which is closer to recent experiments supporting Cu-Zn disorder at all 2a, 2c and 2d sites,[15,16] rather than early experimental suggestions that Cu-Zn disorder occurs only in the Cu-Zn plane.[13,14] Note that such a feature can be easily observed in the occupation variations, whereas conventional temperature evolutions of energy or correlation functions can only provide implicit evidences.

Next, we focus on situations below the transition temperature. Compared to the stoichiometric case, occupations for the Cu poor and Zn rich cases are obviously different. As seen in Fig. 2(a) and 2(d), for the stoichiometric case, Cu and Zn show no preference for 2a and 2c sites below the transition temperature. However, when vacancies are present, Cu prefers occupying a 2a over a 2c site and Zn prefers the opposite. As the proportion of Cu decreases and those of Zn and vacancy increase, the occupation preference at each site becomes more and more obvious. Such site preferences can be understood as follows. First, in the non-stoichiometric samples, we note that vacancies are present at all sites with 2a site slightly favored below the transition temperature. Because 2c and 2d sites have more similar local environments as discussed above, excess Zn after occupying 2d sites is more likely to occupy 2c sites rather than 2a sites. Second, below the transition temperature, we observe large-scale clustering of Zn occupying 2c sites in very large non-stoichiometric supercells during our MC simulations, which could be due to the total energy reductions through defect-defect interactions. Such a phenomenon, however, is difficult to observe in small supercells used in typical first-principles calculations[9] considering just single isolated point defects, indicating the necessity of large-supercell simulations. The site preference of Cu below the transition temperature can be understood as a straightforward consequence of Zn occupation preference. Note that this site preference in non-stoichiometric CZTS can be seen as some new kind of ordering similar to the ordered defect compounds[30,31] in $CuIn_xGa_{1-x}Se_2$, which can affect the electronic properties of CZTS samples, as we will discuss below.

B. Temperature evolution of band gaps in CZTS

After getting the atomic occupation information from MC simulations, we estimate the band gap variations with temperature using an empirical formula proposed in the experiments,[32] which assumes a linear relation between concentrations and band gaps as

$$E_g = E_{g0} + k([A] - [P]). \quad (2)$$

Parameters obtained from the experiments are used, including the band gap of the perfect kesterite structure E_{g0} = 1.59 eV and k = 0.3 eV. $[A]$ and $[P]$ are concentrations of A-type defect pairs ($Zn^{+}_{Cu} + V^{-}_{Cu}$) and P-type defect pairs ($Zn^{+}_{Cu} + Cu^{-}_{Zn}$) in a 16-atom unit cell respectively. To obtain the concentration of A-type defect pairs, we count the number of vacancies at 2a and 2c sites in our MC simulated structures which are originally occupied by Cu, assuming that there are enough Zn_{Cu} to form pairs in the Zn rich conditions. Similarly, for P-type defect pairs we focus on the number of Cu at 2d sites.

The dependence of band gaps on the annealing temperatures and stoichiometry can then be obtained straightforwardly. As shown in Fig. 3, order-disorder transitions are clearly observed in all cases, demonstrating that the band gap can be taken as an effective order parameter as commonly used in experiments.[5,6,32] The band gap decreases with increasing the annealing temperature for all three samples. As temperature increases, the degree of Cu-Zn disorder becomes larger and the band gap therefore decreases. At a fixed temperature either above or below the transition temperature, the

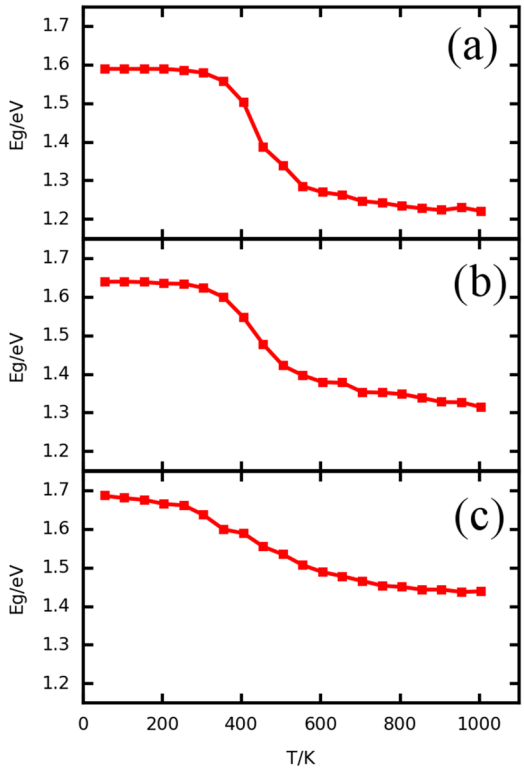

FIG. 3. Estimated band gaps of CZTS from the structures in MC simulations for (a) f_{Cu}=2/3, f_{Zn}=1/3, (b) f_{Cu}=0.58, f_{Zn}=0.38, (c) f_{Cu}=0.50, f_{Zn}=0.42, respectively. Squares are obtained from simulated data and lines are guides for the eye.

band gap increases with the decrease of Cu and increase of Zn and vacancies, consistent with the experiments.[20,21] This can be understood from two aspects. First, more $Zn_{Cu}^{+} + V_{Cu}^{-}$ complexes will form under Cu poor and Zn rich conditions. Because the valence band maximum is formed by the hybridization of Cu-3d and S-3p orbitals, Cu deficiency reduces this hybridization and downshifts the valence band maximum, thus increasing the band gaps.[20,31] Second, as shown in our MC simulations for non-stoichiometric cases, Zn prefers occupying 2c sites over 2a sites below the transition temperature. Such site preferences mean that Cu and Zn are not randomly distributed at 2a and 2c sites but form a more ordered state, and therefore Cu-Zn disorder is suppressed under Cu poor and Zn rich conditions with the increase of band gaps, consistent with the experimental findings.[33]

C. Order-disorder transitions in CZTSe

Following the same procedure, we also analyze the Cu-Zn disorder in CZTSe for which similar order-disorder transitions are observed. The transition temperature is lower than that of CZTS. Several main features of the transition still exist in CZTSe. Above the transition temperature, disorder also appears at 2a sites, though the degree of the disorder is less than those of 2c and 2d sites. Below the transition temperature, excess Zn mainly occupies 2c rather than 2a sites. Following the former approach, we also extract the band gap variations with temperature. The band gap is smaller in CZTSe, but the whole order-disorder transition is similar to that in CZTS. As the concentrations of Zn and vacancies increase, the band gap also increases.

IV. CONCLUSIONS

In conclusion, we have studied the Cu-Zn disorder at Cu-Zn sites (2a, 2c and 2d) both in stoichiometric and non-stoichiometric CZTS/CZTSe using the cluster expansion method and Monte Carlo simulations. By analyzing the structures in MC simulations, we have obtained the temperature evolutions of site occupations from which order-disorder transitions are clearly observed. We find that above the transition temperature, the 2a, 2c, and 2d Wyckoff sites all show disorder in cases both with and without vacancies. However, the degree of disorder at 2a sites is less than that at 2c and 2d sites, indicating an intermediate situation closer to recent experiments supporting Cu-Zn disorder at all 2a, 2c and 2d sites, rather than early experimental suggestions that Cu-Zn disorder occurs only in the Cu-Zn plane. Furthermore, below the transition temperature in the non-stoichiometric cases with vacancies at Cu-Zn sites, excess Zn prefers occupying 2c over 2a sites due to the greater similarity of the 2c site with the 2d site environment. Such site preferences indicate that Cu-Zn occupations exhibit some new kind of ordering rather than randomly distributed at 2a and 2c sites, which is helpful for the increase of the band gaps. We have demonstrated this point by estimating the band gaps, using an empirical formula, of samples annealed at different temperatures based on the site occupation information from MC simulations. Our theoretical studies show that while Cu-Zn disorder reduces the band gap, the site preferences in non-stoichiometric samples increase the band gaps by suppressing Cu-Zn disorder. In general, our work shows that lowering annealing temperatures, increasing Zn and vacancies will lead to larger band gaps. This is helpful for improving solar cell efficiency through careful control of the proportions of the elements in synthesis, and annealing temperatures. The same routines are also suitable for further exploring S-Se disorder at the anionic sites along with disorder at the cationic sites. Understanding the interactions between these two kinds of disorder may shed light on the high efficiency[1] of $Cu_2ZnSn(S,Se)_4$ solar cells.

ACKNOWLEDGMENTS

Y.-F. Zheng would like to thank Prof. Wragg for polishing the manuscript. This work was supported by Science Challenge Project (TZ2018004), National Natural Science Foundation of China (NSFC), National Key Research and Development Program of China (2016YFB0700700) and the Supercomputer Center of Fudan University.

REFERENCES

[1] W. Wang, M. T. Winkler, O. Gunawan, T. Gokmen, T. K. Todorov, Y. Zhu, and D. B. Mitzi, Advanced Energy Materials **4**(7), 1301465 (2014).
[2] M. A. Green, Y. Hishikawa, W. Warta, E. D. Dunlop, D. H. Levi, J. Hohl-Ebinger, and A. W. H. Ho-Baillie, Progress in Photovoltaics: Research and Applications **25**(7), 668–676 (2017).
[3] P. Jackson, R. Wuerz, D. Hariskos, E. Lotter, W. Witte, and M. Powalla, Physica Status Solidi (RRL) – Rapid Research Letters **10**(8), 583–586 (2016).

[4]T. K. Todorov, J. Tang, S. Bag, O. Gunawan, T. Gokmen, Y. Zhu, and D. B. Mitzi, Advanced Energy Materials **3**(1), 34–38 (2013).
[5]G. Rey, A. Redinger, J. Sendler, T. P. Weiss, M. Thevenin, M. Guennou, B. E. Adib, and S. Siebentritt, Applied Physics Letters **105**(11), 112106 (2014).
[6]C. Krämmer, C. Huber, C. Zimmermann, M. Lang, T. Schnabel, T. Abzieher, E. Ahlswede, H. Kalt, and M. Hetterich, Applied Physics Letters **105**(26), 262104 (2014).
[7]T. Gokmen, O. Gunawan, T. K. Todorov, and D. B. Mitzi, Applied Physics Letters **103**(10), 103506 (2013).
[8]S. Schorr, Solar Energy Materials and Solar Cells **95**(6), 1482–1488 (2011).
[9]S. Chen, J.-H. Yang, X. G. Gong, A. Walsh, and S.-H. Wei, Physical Review B **81**(24), 245204 (2010).
[10]A. Walsh, S. Chen, S.-H. Wei, and X.-G. Gong, Advanced Energy Materials **2**(4), 400–409 (2012).
[11]S. Chen, A. Walsh, X.-G. Gong, and S.-H. Wei, Advanced Materials **25**(11), 1522–1539 (2013).
[12]S. P. Ramkumar, A. Miglio, M. J. van Setten, D. Waroquiers, G. Hautier, and G. M. Rignanese, Physical Review Materials **2**(8), 085403 (2018).
[13]J. J. S. Scragg, L. Choubrac, A. Lafond, T. Ericson, and C. Platzer-Björkman, Applied Physics Letters **104**(4), 041911 (2014).
[14]A. Ritscher, M. Hoelzel, and M. Lerch, Journal of Solid State Chemistry **238**, 68–73 (2016).
[15]C. J. Bosson, M. T. Birch, D. P. Halliday, K. S. Knight, A. S. Gibbs, and P. D. Hatton, Journal of Materials Chemistry A **5**(32), 16672–16680 (2017).
[16]C. J. Bosson, M. T. Birch, D. P. Halliday, C. C. Tang, A. K. Kleppe, and P. D. Hatton, Chemistry of Materials **29**(22), 9829–9839 (2017).
[17]K. Yu and E. A. Carter, Chemistry of Materials **28**(3), 864–869 (2016).
[18]J. M. Sanchez, F. Ducastelle, and D. Gratias, Physica A: Statistical Mechanics and its Applications **128**(1), 334–350 (1984).
[19]T. K. Todorov, K. B. Reuter, and D. B. Mitzi, Advanced Materials **22**(20), E156–E159 (2010).
[20]M. Lang, T. Renz, N. Mathes, M. Neuwirth, T. Schnabel, H. Kalt, and M. Hetterich, Applied Physics Letters **109**(14), 142103 (2016).
[21]M. V. Yakushev, M. A. Sulimov, J. Márquez-Prieto, I. Forbes, J. Krustok, P. R. Edwards, V. D. Zhivulko, O. M. Borodavchenko, A. V. Mudryi, and R. W. Martin, Solar Energy Materials and Solar Cells **168**, 69–77 (2017).
[22]A. van de Walle, Calphad-Computer Coupling of Phase Diagrams and Thermochemistry **33**(2), 266–278 (2009).
[23]A. v. d. Walle and M. Asta, Modelling and Simulation in Materials Science and Engineering **10**(5), 521 (2002).
[24]A. van de Walle and G. Ceder, Journal of Phase Equilibria **23**(4), 348 (2002).
[25]G. Kresse and J. Furthmüller, Physical Review B **54**(16), 11169–11186 (1996).
[26]G. Kresse and J. Furthmüller, Computational Materials Science **6**(1), 15–50 (1996).
[27]P. E. Blöchl, Physical Review B **50**(24), 17953–17979 (1994).
[28]G. Kresse and D. Joubert, Physical Review B **59**(3), 1758–1775 (1999).
[29]J. P. Perdew, K. Burke, and M. Ernzerhof, Physical Review Letters **77**(18), 3865–3868 (1996).
[30]S. B. Zhang, S. H. Wei, A. Zunger, and H. Katayama-Yoshida, Physical Review B **57**(16), 9642–9656 (1998).
[31]S. H. Wei, S. B. Zhang, and A. Zunger, Applied Physics Letters **72**(24), 3199–3201 (1998).
[32]M. Valentini, C. Malerba, F. Menchini, D. Tedeschi, A. Polimeni, M. Capizzi, and A. Mittiga, Applied Physics Letters **108**(21), 211909 (2016).
[33]M. Paris, L. Choubrac, A. Lafond, C. Guillot-Deudon, and S. Jobic, Inorganic Chemistry **53**(16), 8646–8653 (2014).